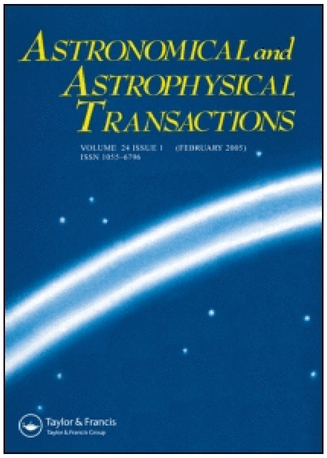

Astronomical & Astrophysical Transactions
The Journal of the Eurasian Astronomical Society
Publication details, including instructions for authors and subscription information:
http://www.informaworld.com/smpp/title~content=t713453505

Dust in the expanding wolf-rayetstar atmospheres. II. Themicrostructure theory of the dustshell and the infrared spectra modelling

V. G. Zubko [a]
[a] Main Astronomical Observatory of the Ukrainian Academy of Sciences, Kiev, Ukraine

Online Publication Date: 01 January 1992
To cite this Article: Zubko, V. G. (1992) 'Dust in the expanding wolf-rayetstar atmospheres. II. Themicrostructure theory of the dustshell and the infrared spectra modelling', Astronomical & Astrophysical Transactions, 3:2, 141 - 152
To link to this article: DOI: 10.1080/10556799208230551
URL: http://dx.doi.org/10.1080/10556799208230551

Astronomical and Astrophysical Transactions, 1992,
Vol. 3, pp. 141–152
Reprints available directly from the publisher.
Photocopying permitted by license only

DUST IN THE EXPANDING WOLF–RAYET STAR ATMOSPHERES. II. THE MICROSTRUCTURE THEORY OF THE DUST SHELL AND THE INFRARED SPECTRA MODELLING

V. G. ZUBKO

Main Astronomical Observatory of the Ukrainian Academy of Sciences,
Goloseyevo Forest, Kiev, 252127, Ukraine

(Received 23 October, 1991; in final form December 9, 1991)

A simple theory of the microstructure of WR star dust shells is proposed. Under some plausible assumptions, an analytic solution of the kinetic equation for the dust grain distribution function is obtained. It is shown that the WC star infrared spectrum calculated from the theory can be adjusted to agree with observations in the case of graphite (not amorphous) dust grains. The nucleation rate and other parameters of the dust shell are estimated under the assumption that the grain growth occurs via the implantation of impinging carbon ions into the dust particles.

KEY WORDS WR stars, infrared spectra, dust shells.

1. INTRODUCTION

The problem of dust formation and survival is one of the most intriguing problems in the WR star astrophysics. Already the infrared photometric investigations of Allen *et al.* (1972), Gehrz and Hackwell (1974) and Cohen *et al.* (1975) showed the presence of dust around the latest subtypes of WC stars. It has been found later that the stars earlier than WC8 have no permanent dust envelopes (Pitault *et al.*, 1983). The extended infrared photometry by Williams *et al.* (1987) of galactic population I WC8-10 stars resulted in the discovery of a heated dust around these stars. The episodic dust condensations have been detected around two WC7 stars: WR137 in 1984 (Williams *et al.*, 1985) and WR140 in 1977 (Williams *et al.*, 1978; Hackwell *et al.*, 1979) and in 1985 (Williams *et al.*, 1990). Moreover, recently Williams *et al.* (1990) observed episodical dust in the WR19 star classified as WC4 in the Catalogue of WR stars (van der Hucht *et al.*, 1981). Thus, the dust condensation can take place even in the stellar winds of the earliest subtypes. How these observations can be explained? For the permanent dust around WC8-10 stars, Williams *et al.* (1987) proposed dust shell models with spherical symmetry, an inverse square law for the dust density distribution, and amorphous carbon as the dust material. These models provide a good fit to the observed infrared spectra of WC8-10 but they are physically unrealistic due to the adopted artificial dust density distribution.

Moreover, it is obvious that traditional dust condensation theories cannot account for both the dust nucleation and the subsequent dust nuclei growth in the severe conditions of WR winds. In our previous paper (Zubko *et al.*, 1992) we proposed and modelled a possible mechanism of carbon dust grain growth in a WR shell due to collisions with positive carbon ions. In the present paper, we develop further this idea. In Section 2 we derive the kinetic equation for the dust distribution function and solve it analytically. In Section 3 we derive expressions for the luminosities of the dust shell. In Section 4 we propose a physical criterion for choosing the carbon material from which the grains are formed, either graphite or amorphous carbon. And, finally, in Section 5 we analyze the resulting infrared spectra and estimate dust shell parameters for a group of WR stars. It is to be noted that the question of the nucleation mechanism remains to be open, but the proposed fitting procedure allows us to calculate the nucleation rate and distance.

2. KINETIC EQUATION FOR THE DUST DISTRIBUTION FUNCTION

Following our previous paper (Zubko *et al.*, 1992), we shall use the following equations governing physical parameters of an individual dust grain embedded in the wind of a WR star:

$$\frac{dR}{dt} = v + u, \tag{1}$$

$$u \sum_k m_k n_k \frac{8}{3\sqrt{\pi}} \left(\frac{9\pi}{64} u^2 + \frac{2kT}{m_k} \right)^{1/2} = \frac{1}{c} \left(\frac{R_*}{R} \right)^2 \bar{Q}(a, T_*) \sigma T_*^4, \tag{2}$$

$$\frac{da}{dt} = \Omega \left[\sum_k \left[\frac{n_k^c}{4} \left(u^2 + \frac{8kT}{\pi m_c} \right)^{1/2} \left(1 - \frac{2 z_k e U}{m_c u^2} \right) (s_k - y_k) \right] - \frac{p_s(T_d)}{(2\pi m_c k T_d)^{0.5}} \right], \tag{3}$$

$$N_e \left(\frac{8kT_e}{\pi m_e} \right)^{1/2} \left(1 + \frac{eU}{kT_e} \right) = \int_{\nu_0}^{\infty} \frac{J_\nu}{h\nu} Q_\nu y_\nu \, d\nu + J_i, \tag{4}$$

$$4\bar{Q}(a, T_d) \sigma T_d^4 = \left(\frac{R_*}{R} \right)^2 \bar{Q}(a, T_*) \sigma T_*^4, \tag{5}$$

where all the notation and definitions are the same as in Zubko *et al.* (1992). Basing on this system of equations, one can consider an ensemble of dust grains. Assuming spherical symmetry and quasi-steady state, the distribution function $\varphi(R, a)$ can be introduced, which is the number density of dust grains of the size a at the distance R from the star. If the diffusion and coagulation of dust grains are negligible (this is the case for the conditions in the WR wind), then the kinetic equation has the form

$$\frac{1}{R^2} \frac{\partial}{\partial R} \left(R^2 \frac{dR}{dt} \varphi \right) + \frac{\partial}{\partial a} \left(\frac{da}{dt} \varphi \right) = J(R)\, \delta(a - a_0(R)), \tag{6}$$

where $J(R)$ is the nucleation rate, $a_0(R)$ is the condensation nucleus radius at the distance R and δ is Dirac's delta-function. Equations (6) and (1)–(5) are complicated enough as to justify some simplifications in order to obtain an analytic solution. Firstly, we adopt an inverse square law for the number density distributions of all plasma components, in accordance with the assumption $v = \text{const}$ for $R > 100R_*$. Secondly, we can ignore the evaporation term in Eq. (3). The results of model calculations (Section 5) confirm this simplification: the ratio of the thermal evaporation rate to the growth rate does not exceed 10^{-8}–10^{-6}. It should be noted that these simplifications are not used in the final model calculations but only applied to solve the kinetic equation.

Concerning the problem of the dust grain material, it should be noted that, following Williams *et al.* (1987), our original presumption was that the dust consists of amorphous carbon. But the estimations of the characteristic condensation time (Section 4) and the comparison with infrared observations of WC stars (Section 5) showed that this is not the case. A more suitable substance is graphite.

Using the technique of Draine and Lee (1984), we calculated the optical properties of graphite including the dielectric constant ε, and extinction efficiencies $Q_\lambda(a)$ and $\bar{Q}(a, T)$ for high-temperature region $T = 300$–1800 K and for the size range $a = 0.0004$–$0.02\ \mu$m typical of dust grains in the WR shells. It should be noted that the original results of Draine and Lee (1984) are valid only for the temperatures below 300 K. In our calculations, we used the conductivity data for pure graphite from Kikoin (1976).

After some simplifications, we obtain

$$\frac{dR}{dt} = g(a), \tag{7}$$

$$\frac{da}{dt} = \frac{f(a)}{R^2}, \tag{8}$$

where functions $f(a)$ and $g(a)$ have the form:

$$g(a) = v + u(a), \tag{9}$$

$$f(a) = \tfrac{1}{4}\Omega R_*^2 \left(u^2(a) + \frac{8kT}{\pi m_c}\right)^{1/2} \sum_k n^c_{k_0}\left(1 - \frac{2z_k eU(a)}{m_c u^2(a)}\right)(s_k - y_k(a), \tag{10}$$

where $n^c_{k_0}$ is the number density of carbon ions at distance R_*.

Thus, we have to solve the kinetic equation (6) together with equations (7)–(10) and with the boundary condition $\varphi = 0$ (no dust grains) at the inner edge of the dust shell R_1. Using the technique of characteristics it is easy to obtain first integrals:

$$F(a) + \frac{1}{R} = C_1, \qquad F(a) = \int \frac{g(a)}{f(a)}\, da, \tag{11}$$

$$f(a)R^2\varphi - \int_{R_1}^{R} \left[\frac{J(R')R'^2}{g(a(R'))} - f(a(R'))\ \delta(a(R') - a_0(R'))\right] dR' = C_2. \tag{12}$$

Since $\varphi = 0$ at the inner edge R_1, we obtain $C_2 = 0$ and

$$\varphi(R, a) = \frac{1}{R^2 f(a)} \int \left[\frac{J(R')R'^2}{g(a(R'))} f(a(R'))\ \delta(a(R') - a_0(R'))\right] dR'. \tag{13}$$

Inserting here $a(R')$ from the first integral (11) in the form

$$a(R') = F^{-1}\left(F(a) + \frac{1}{R} - \frac{1}{R'}\right) \equiv \Phi(a, R, R'), \tag{14}$$

where F^{-1} is the inverse function to F and employing the delta-function property

$$\delta[x(a)] = \frac{\delta(a - a_*)}{x'_a(a_*)}, \tag{15}$$

where a_* is a simple root of equation $x(a) = 0$, we obtain after some transformations that

$$\varphi(R, a) = \frac{1}{R^2 f(a)} \times \int_{R_1}^{R} dR' R'^2 J(R') \frac{f(a_*) f(\Phi(a, R, R')) g(\Phi(a_*, R, R'))}{g(a_*) f(\Phi(a_*, R, R')) g(\Phi(a, R, R'))} \delta(a - a_*), \tag{16}$$

$$a_* = \Phi(a_0(R'), R', R). \tag{17}$$

Changing the integration variable in (16) from R' to a_* and integrating (16) we obtain

$$\varphi(R, a) = \frac{J(R_0)}{g(a)} \frac{R_0^2}{R^2} \frac{1}{-\left(\dfrac{\partial a_*}{\partial R'}\right)_{R'=R_0}}, \tag{18}$$

where R_0 is the nucleation distance for a dust grain of the size a at the distance R:

$$\frac{1}{R_0} = \frac{1}{R} + F(a) - F(a_0). \tag{19}$$

It is easy to calculate the derivative of a_* with respect to R' in Eq. (18) using the assumption that the nucleation radius a_0 is constant throughout the nucleation zone:

$$-\left(\frac{\partial a_*}{\partial R'}\right)_{R'=R_0} = \frac{1}{R_0} \frac{f(a)}{g(a)}. \tag{20}$$

Thus, we obtain the following final form for $\varphi(R, a)$:

$$\varphi(R, a) = \frac{J(R_0) R_0^2}{f(a)} \left(\frac{R_0}{R}\right)^2. \tag{21}$$

It can be seen that this dust distribution law (21) is basically different from the inverse square law adopted by Williams *et al.* (1987), with the factor $1/f(a)$. As we shall see below, this difference is decisive for the choice of the dust material (either graphite or amorphous carbon) which is made using fitting calculations of WC infrared spectra (see Section 5).

3. THE LUMINOSITY OF THE DUST SHELL

It is convenient to use for further analysis the moments of the distribution function $\varphi(R, a)$ defined as

$$\varphi_n(R) = \int_0^\infty a^n \varphi(R, a)\, da. \tag{22}$$

Using in (22) the form (16) for $\varphi(R, a)$, we obtain

$$\varphi_n(R) = \int_{R_1}^{R} dR' J(R') \left(\frac{R'}{R}\right)^2 \frac{a_*^n}{g(a_*)}. \tag{23}$$

Here we used the assumption that dust nucleation takes place in a thin layer of thickness $\Delta R_0 \ll R_0$ located at distance R_0 from the star. The corresponding nucleation rate and radius of nuclei are denoted by J_0 and a_0, respectively. Using this assumption, we obtain from (23):

$$\varphi_n(R) = \left(\frac{R_0}{R}\right)^2 J_0\, \Delta R_0 \frac{a(R)^n}{g(a(R))}. \tag{24}$$

If the dust shell is optically thin (this assumption is confirmed by our calculations) and the dust grain radiates according to the Planck law with the absorbtion efficiency Q_λ, then the dust shell luminosity is given by

$$L_\lambda^d = \int_{R_0}^\infty 4\pi R^2\, dR \int_0^\infty 4\pi a^2 Q_\lambda(a, T_d) \pi B_\lambda(T_d(R)) \varphi(R, a)\, da, \tag{25}$$

where B_λ is the Planck function

$$B_\lambda(T_d(R)) = \frac{2hc^2}{\lambda^5}\left(\exp\left(\frac{hc}{kT_d(R)}\right) - 1\right)^{-1}. \tag{26}$$

For further applications, it is convenient to represent the graphite absorbtion efficiency $Q_\lambda(a, T_d)$ in the infrared region $\lambda > 0.8\,\mu\text{m}$ as

$$Q_\lambda(a, T_d) = \frac{A_1}{\lambda^{A_2}} a, \tag{27}$$

where A_1 and A_2 are tabulated functions which depend on the graphite grain temperature T_d and the grain size a. We should note that the dependence of both A_1 and A_2 on a is very weak. Allowing for this and using equation (24) with $n = 3$, we obtain from (25):

$$\begin{aligned} L_\lambda^d &= 16\pi^3 \int_{R_0}^\infty dR R^2 B_\lambda(T_d(R)) \frac{A_1}{\lambda^{A_2}} \int_0^\infty da\, a^3 \varphi(R, a) \\ &= 16\pi^3 J_0 R_0^2\, \Delta R_0 \int_{R_0}^\infty dR\, B_\lambda(T_d(R)) \frac{A_1}{\lambda^{A_2}} \frac{a^3(R)}{g(a(R))}. \end{aligned} \tag{28}$$

Equation (28) is used to calculate the model spectra of dust shells.

Since IR-observations are often done with different diaphragms at the different wavelengths and we have already pointed out the importance of the "diaphragm" effect (Zubko *et al.*, 1992), a correction for this effect should be introduced in Eq. (28) before comparing it with observations. If D_λ is the "diaphragm" radius at wavelength λ, the integration operator in (28) has to be replaced by the following operators depending on the values of R_0 and D_λ:

$$D_\lambda < R_0: \int_{R_0}^{\infty} dR \ldots \rightarrow \int_{R_0}^{\infty} dR\left(1-\left(1-\frac{D_\lambda^2}{R^2}\right)^{1/2}\right) \ldots, \tag{29}$$

$$D_\lambda > R_0: \int_{R_0}^{\infty} dR \ldots \rightarrow \int_{D_\lambda}^{\infty} dR\left(1-\left(1-\frac{D_\lambda^2}{R^2}\right)^{1/2}\right) \ldots + \int_{R_0}^{D_\lambda} dR \ldots. \tag{30}$$

The total luminosity of the dust shell is given by

$$L^d = \int_{R_0}^{\infty} 4\pi R^2\, dR \int_0^{\infty} 4\pi a^2 \bar{Q}(a, T_d)\sigma T_d^4 \varphi(R, a)\, da. \tag{31}$$

The mean Planck efficiency for graphite $\bar{Q}(a, T_*)$ can be represented in the ultraviolet region $\lambda < 0.2\ \mu$m as

$$\bar{Q}(a, T_*) = A_3 a T_*^{A_4}, \tag{32}$$

where A_3 and A_4 are slowly varying with a and T_d. After substituting Eqs (5), (32) and (24) in Eq. (31) and some transformations we obtain:

$$L^d = 4\pi^2 R_*^2 A_3 \sigma T_*^{4+A_4} J_0 R_0^2\, \Delta R_0 \int_{R_0}^{\infty} \frac{dR}{R^2} \frac{a^3(R)}{g(a(R))}. \tag{33}$$

The ratio of the dust luminosity L^d to the stellar luminosity $L^* = 4\pi R_*^2 \sigma T_*^4$ is

$$\frac{L^d}{L^*} = \pi A_3 T_*^{A_4} J_0 R_0^2\, \Delta R_0 \int_{R_0}^{\infty} \frac{dR}{R^2} \frac{a^3(R)}{g(a(R))}. \tag{34}$$

4. GRAPHITE OR AMORPHOUS CARBON?

Gail and Sedlmayr (1984) proposed a rough physical criterion to decide what is the material of the grains, graphite or amorphous carbon. They introduced the surface hopping time t_h (the settled lifetime of an impinged carbon ion at the dust grain surface before it jumps to a lattice site) and the mean capture time t_c (the time between two subsequent successful stickings of impinging carbon ions to the dust grain). It is clear that a crystalline carbon (graphite) grain starts to grow when $t_c/t_h \gg 1$ because in this case the incident carbon ion will be imbeded into the crystalline lattice prior to the next ion impinging and otherwise, an amorphous carbon grain starts to grow if $t_c/t_h \ll 1$.

For t_h Gail and Sedlmayr (1984) propose the following expression:

$$t_h = \frac{1}{\nu_0} \exp\left(\frac{U_b}{kT_d}\right), \tag{35}$$

where ν_0 is the carbon ion mean oscillation frequency at a settled place and U_b is the mean surface-energy barrier for the migration along the dust grain surface. We adopt $\nu_0 = 3.8 \cdot 10^{12}\ \mathrm{s}^{-1}$ and $U_b = 2.9$ eV (Gail and Sedlmayr, 1984).

However, the expression for t_c obtained by Gail and Sedlmayr (1984) is inapplicable here because it is valid only in the case of the Maxwell distribution of gas particles colliding with the dust grain. In our case, the dust grains move in plasma environment at supersonic velocity and we can write:

$$t_c = \frac{\Omega}{4\pi a^2} \frac{1}{\left.\frac{da}{dt}\right|_+}, \tag{36}$$

where $da/dt|_+$ (the term on the right-hand side of Eq. (3) responsible for the grain growth) is proportional to the mean thermal velocity of plasma particles in the Maxwellian limit and da/dt is proportional to the drift velocity of a dust grain within the shell in the highly supersonic limit.

Our calculations of the WC dust shell models show that $t_c/t_h \gg 1$, that is, graphite dust grains can grow. This conclusion is in agreement with the fitting results (see Section 5).

5. RESULTS OF THE DUST SHELL SPECTRA MODELLING

We attempted to model the IR-spectra of eight late WC stars: WR69, WR70, WR76, WR80, WR95, WR96, WR118 and WR48a using the corresponding data of Williams *et al.* (1987) and Danks *et al.* (1983). We are based on the assumptions, ideas and formulae described by Zubko *et al.* (1992) and the above arguments. It has been adopted that the shell velocity, v, is 2000 km/s; the gas temperature in the shell, T, is 10000 K; the mass loss rate is $\dot{M}_* = 8 \cdot 10^{-5} M_\odot/\text{year}$; the stellar radius is $10\,R_\odot$; the chemical composition (by mass) is: $C/\text{He} = 0.9$ and $O/\text{He} = 0.08$ (this is typical of the late WC stars—Nugis, 1991); the photoelectric efficiency g is 0.01 (Williams *et al.*, 1987); the sticking probability s is 1.0 (we supposed that carbon ions are implanted into the dust grains with the probability about 1); the effective stellar temperature, T_*, is 26000 K for WC8 stars, 22000 K for WC9 stars and 20000 K for WC10 stars (Williams *et al.*, 1987). The variable parameter is the nucleation distance R_0. We have calculated the dynamics, growth and the dust shell luminosities using Eqs. (1–5), (7–10), (28–30), and (34–36). To find the total luminosity, the stellar luminosity and the free-free luminosity of the stellar wind should be calculated. But for WR stars, these luminosities are interconnected and to calculate the "star + wind" luminosity we used the theory of Nugis (1977).

It has been adopted that the radius of condensation nuclei equals 0.0004 μm.

The fitting technique is the following: at the first stage we calculate the dust shell model and all the luminosities; at the second stage, it is necessary to calibrate all the luminosities using the observed optical (b, v) data; and at the third stage, we vary $J_0\,\Delta R_0$ in Eq. (28) for the dust shell luminosity in order to obtain the best fit.

The main results of our calculations are presented in Table 1 where the names of WR stars in the first column refer to the Catalogue of WR stars of van der Hucht *et al.* (1981); T_* is the stellar effective temperature in 1000 K; L_d/L with (*) is the ratio of the dust shell luminosity to the total luminosity expressed in per cent, according to Williams *et al.* (1987); L_d/L is the same ratio from our

Table 1 The calculated parameters of WC star dust shells.

Star	T_*	$L_d/L_{(*)}$	L_d/L	$\frac{N_d}{N}$	R_0	T_{d0}	$J_0\,\Delta R_0$	a_f	$\bar{m}$
WR	10^3 K	%	%	%	R_s	K	$\mathrm{cm}^{-2}\,\mathrm{s}^{-1}$	nm	%
48	26	54	63	4.2	1870	1134	$1.5\cdot10^5$	2.7	3.0
69	22	2.0	1.6	0.02	645	1008	$4.0\cdot10^4$	6.1	6.5
70	26	0.6	0.8	0.03	2620	1283	$5.8\cdot10^4$	2.7	6.4
76	22	68	71	3.7	902	1266	$4.8\cdot10^6$	6.1	3.1
80	22	9.6	9.9	0.12	711	1375	$2.5\cdot10^6$	6.1	4.0
95	22	3.7	4.2	0.04	602	1458	$1.2\cdot10^5$	6.1	6.0
96	22	9.5	9.7	0.1	613	1448	$2.8\cdot10^5$	6.1	4.2
118	20	71	74	3.8	659	1300	$2.3\cdot10^6$	9.8	5.0

Note: For WR48a, the model applies to the 1979.5 data of Danks *et al.* (1983).

calculations; N_d/N is the ratio of the number of solid carbon atoms to that of gaseous carbon in per cent; R_0 is the nucleation distance in R_*; T_{d0} is the dust temperature at R_0 in K; $J_0\,\Delta R_0$ is measured in $\mathrm{cm}^{-2}\,\mathrm{s}^{-1}$; a_f is the final size of a dust grain in nm; $\bar{m}$ is the root-mean-square fitting error in per cent.

The dust shell models for all the considered stars are presented in Tables 2–9 where R is the distance of the dust shell to the star in R_*; a is the dust grain radius in nm; T_d is the temperature of a dust grain in K; u is the drift velocity of a dust grain in km/s; t_c/t_h is the ratio of the characteristic condensation times (see Section 4); y is the mean sputtering yield for the incident ions on a dust grain, measured in the number of sputtered atoms (or ions) per incident ion; A_1 and A_2 are the parameters appearing in Eq. (27) for the absorbtion efficiency of a graphite grain with a and λ measured in μm. It can be seen that $t_c/t_h > 1$ in the zone of intensive dust grain growth for practically all analyzed stars and, as a consequence, graphite dust grains should start to grow. However, at far distances from the star, an amorphous carbon mantle may grow as well. As a rule, the mantle is too thin for producing a visible effect in the dust shell spectrum.

The mechanism of the dust grain growth is the collisions with impinging carbon

Table 2 The dust shell model for the WR69 star (WC9).

R	a	T_d	u	t_c/t_h	y	A_1	A_2
645	0.4	1422	19.2	$2.8\cdot10^5$	0.0	3.32	1.73
647	0.4	1421	20.2	$2.1\cdot10^5$	0.0	3.28	1.71
654	0.6	1418	23.6	$9.6\cdot10^4$	0.0	3.19	1.69
674	1.3	1405	34.1	$1.3\cdot10^4$	$2.3\cdot10^{-2}$	3.00	1.63
740	3.8	1361	58.9	$4.7\cdot10^2$	$4.6\cdot10^{-1}$	2.83	1.57
948	5.9	1243	73.5	$2.4\cdot10^1$	$9.5\cdot10^{-1}$	2.79	1.54
1610	6.1	1027	74.7	$2.2\cdot10^{-1}$	1.0	2.79	1.54
3700	6.1	760	74.7	$1.2\cdot10^{-5}$	1.0	2.78	1.54
10300	6.1	525	74.7	$2.2\cdot10^{-13}$	1.0	2.77	1.54
31200	6.1	352	74.7	$\ll1$	1.0	2.77	1.53
97400	6.1	233	74.7	$\ll1$	1.0	2.76	1.53
307000	6.1	154	74.7	$\ll1$	1.0	2.76	1.53
968000	6.1	101	74.7	$\ll1$	1.0	2.76	1.53

Table 3 The dust shell model for the WR76 star (WC9).

R	a	T_d	u	t_c/t_h	y	A_1	A_2
902	0.4	1266	19.2	$3.0 \cdot 10^4$	0.0	3.31	1.72
904	0.4	1265	19.7	$2.5 \cdot 10^4$	0.0	3.30	1.72
910	0.5	1261	21.4	$1.6 \cdot 10^4$	0.0	3.29	1.72
931	0.8	1252	26.7	$4.5 \cdot 10^3$	$5.3 \cdot 10^{-4}$	3.18	1.68
996	2.0	1224	42.6	$2.7 \cdot 10^2$	$1.1 \cdot 10^{-1}$	2.82	1.57
1200	4.9	1141	66.6	$5.7 \cdot 10^0$	$7.1 \cdot 10^{-1}$	2.79	1.54
1860	6.0	974	74.1	$5.2 \cdot 10^{-2}$	$9.8 \cdot 10^{-1}$	2.79	1.54
3960	6.1	742	74.6	$4.6 \cdot 10^{-6}$	1.0	2.78	1.54
10600	6.1	520	74.7	$1.3 \cdot 10^{-13}$	1.0	2.77	1.54
31500	6.1	350	74.7	$\ll 1$	1.0	2.77	1.53
97600	6.1	233	74.7	$\ll 1$	1.0	2.76	1.53
307000	6.1	154	74.7	$\ll 1$	1.0	2.76	1.53
968000	6.1	101	74.7	$\ll 1$	1.0	2.76	1.53

Table 4 The dust shell model for the WR80 star (WC9).

R	a	T_d	u	t_c/t_h	y	A_1	A_2
711	0.4	1375	19.2	$1.5 \cdot 10^5$	0.0	3.32	1.73
713	0.4	1374	20.1	$1.2 \cdot 10^5$	0.0	3.31	1.72
719	0.6	1370	22.8	$6.0 \cdot 10^4$	0.0	3.28	1.71
740	1.1	1359	31.5	$1.0 \cdot 10^4$	$1.1 \cdot 10^{-2}$	3.04	1.64
805	3.2	1320	54.1	$4.0 \cdot 10^2$	$3.3 \cdot 10^{-1}$	2.83	1.57
1010	5.7	1214	72.3	$1.6 \cdot 10^1$	$9.1 \cdot 10^{-1}$	2.79	1.54
1670	6.1	1012	74.6	$1.5 \cdot 10^{-1}$	1.0	2.79	1.54
3770	6.1	756	74.7	$9.3 \cdot 10^{-6}$	1.0	2.78	1.54
10400	6.1	524	74.7	$1.9 \cdot 10^{-13}$	1.0	2.77	1.54
31300	6.1	351	74.7	$\ll 1$	1.0	2.77	1.53
97400	6.1	233	74.7	$\ll 1$	1.0	2.76	1.53
307000	6.1	154	74.7	$\ll 1$	1.0	2.76	1.53
968000	6.1	101	74.7	$\ll 1$	1.0	2.76	1.53

Table 5 The dust shell model for the WR95 star (WC9).

R	a	T_d	u	t_c/t_h	y	A_1	A_2
602	0.4	1458	19.2	$4.4 \cdot 10^5$	0.0	3.33	1.73
604	0.5	1456	20.4	$3.1 \cdot 10^5$	0.0	3.32	1.73
610	0.6	1452	24.2	$1.3 \cdot 10^5$	0.0	3.20	1.69
631	1.4	1440	36.4	$1.5 \cdot 10^4$	$3.9 \cdot 10^{-2}$	2.93	1.60
696	4.2	1391	62.2	$5.4 \cdot 10^2$	$5.6 \cdot 10^{-1}$	2.81	1.56
905	6.0	1265	74.0	$3.4 \cdot 10^1$	$9.7 \cdot 10^{-1}$	2.79	1.55
1570	6.1	1037	74.7	$2.9 \cdot 10^{-1}$	1.0	2.79	1.54
3660	6.1	764	74.7	$1.4 \cdot 10^{-5}$	1.0	2.78	1.54
10300	6.1	526	74.7	$2.4 \cdot 10^{-13}$	1.0	2.77	1.54
31200	6.1	352	74.7	$\ll 1$	1.0	2.77	1.53
97300	6.1	233	74.7	$\ll 1$	1.0	2.76	1.53
306000	6.1	154	74.7	$\ll 1$	1.0	2.76	1.53
968000	6.1	101	74.7	$\ll 1$	1.0	2.76	1.53

Table 6 The dust shell model for the WR96 star (WC9).

R	a	T_d	u	t_c/t_h	y	A_1	A_2
613	0.4	1448	19.2	$3.9 \cdot 10^5$	0.0	3.33	1.73
615	0.5	1448	20.4	$2.9 \cdot 10^5$	0.0	3.26	1.71
621	0.6	1444	24.1	$1.2 \cdot 10^5$	0.0	3.17	1.68
642	1.4	1431	35.8	$1.4 \cdot 10^4$	$3.4 \cdot 10^{-2}$	2.95	1.61
707	4.1	1383	61.4	$5.2 \cdot 10^2$	$5.4 \cdot 10^{-1}$	2.81	1.56
916	6.0	1260	73.8	$3.2 \cdot 10^1$	$9.7 \cdot 10^{-1}$	2.79	1.55
1580	6.1	1035	74.7	$2.7 \cdot 10^{-1}$	1.0	2.79	1.54
3670	6.1	763	74.7	$1.3 \cdot 10^{-5}$	1.0	2.78	1.54
10300	6.1	525	74.7	$2.3 \cdot 10^{-13}$	1.0	2.77	1.54
31200	6.1	352	74.7	$\ll 1$	1.0	2.77	1.53
97300	6.1	233	74.7	$\ll 1$	1.0	2.76	1.53
307000	6.1	154	74.7	$\ll 1$	1.0	2.76	1.53
968000	6.1	101	74.7	$\ll 1$	1.0	2.76	1.53

Table 7 The dust shell model for the WR48a star (WC8)

R	a	T_d	u	t_c/t_h	y	A_1	A_2
1874	0.4	1134	29.1	$3.9 \cdot 10^3$	$2.2 \cdot 10^{-3}$	3.29	1.72
1881	0.4	1134	29.4	$3.7 \cdot 10^3$	$2.7 \cdot 10^{-3}$	3.29	1.72
1889	0.4	1132	30.3	$3.0 \cdot 10^3$	$4.6 \cdot 10^{-3}$	3.26	1.71
1900	0.5	1128	33.2	$1.7 \cdot 10^3$	$1.5 \cdot 10^{-2}$	3.17	1.68
1970	0.8	1114	42.1	$4.0 \cdot 10^2$	$8.9 \cdot 10^{-2}$	3.07	1.65
2170	1.8	1075	60.9	$2.5 \cdot 10^1$	$5.0 \cdot 10^{-1}$	2.97	1.62
2830	2.6	977	73.5	$7.2 \cdot 10^{-1}$	$9.3 \cdot 10^{-1}$	2.85	1.58
4930	2.7	800	75.1	$9.9 \cdot 10^{-4}$	1.0	2.83	1.57
11500	2.7	589	75.2	$1.6 \cdot 10^{-9}$	1.0	2.82	1.56
32500	2.7	405	75.2	$7.2 \cdot 10^{-20}$	1.0	2.80	1.55
98600	2.7	272	75.2	$\ll 1$	1.0	2.80	1.56
308000	2.7	179	75.2	$\ll 1$	1.0	2.76	1.54
969000	2.7	119	75.2	$\ll 1$	1.0	2.77	1.54

Table 8 The dust shell model for the WR70 star (WC8)

R	a	T_d	u	t_c/t_h	y	A_1	A_2
2625	0.4	1008	29.1	$1.9 \cdot 10^2$	$2.2 \cdot 10^{-3}$	3.28	1.71
2632	0.4	1008	29.2	$1.8 \cdot 10^2$	$2.5 \cdot 10^{-4}$	3.28	1.71
2639	0.4	1007	29.7	$1.6 \cdot 10^2$	$3.3 \cdot 10^{-3}$	3.27	1.71
2650	0.5	1004	31.2	$1.2 \cdot 10^2$	$7.0 \cdot 10^{-3}$	3.24	1.70
2720	0.6	995	35.8	$4.5 \cdot 10^1$	$2.9 \cdot 10^{-2}$	3.15	1.68
2920	1.1	968	48.3	$4.5 \cdot 10^0$	$1.9 \cdot 10^{-1}$	3.00	1.63
3580	2.1	898	66.9	$9.1 \cdot 10^{-2}$	$7.0 \cdot 10^{-1}$	2.86	1.58
5670	2.6	762	74.1	$1.7 \cdot 10^{-4}$	$9.6 \cdot 10^{-1}$	2.85	1.58
12300	2.7	576	75.0	$5.0 \cdot 10^{-10}$	$9.9 \cdot 10^{-1}$	2.82	1.57
33200	2.7	402	75.1	$3.9 \cdot 10^{-20}$	1.0	2.80	1.56
99400	2.7	271	75.1	$\ll 1$	1.0	2.80	1.56
309000	2.7	179	75.2	$\ll 1$	1.0	2.76	1.54
970000	2.7	119	75.2	$\ll 1$	1.0	2.77	1.54

Table 9 The dust shell model for the WR69 star (WC10)

R	a	T_d	u	t_c/t_h	y	A_1	A_2
659	0.4	1300	15.1	$4.0 \cdot 10^4$	0.0	3.31	1.72
661	0.4	1298	15.8	$3.2 \cdot 10^4$	0.0	3.29	1.72
667	0.6	1294	17.7	$1.7 \cdot 10^4$	0.0	3.23	1.70
687	1.0	1282	23.9	$3.1 \cdot 10^3$	0.0	3.04	1.64
752	3.1	1242	41.8	$9.7 \cdot 10^1$	$1.0 \cdot 10^{-1}$	2.83	1.57
960	7.8	1135	66.6	$1.2 \cdot 10^0$	$7.1 \cdot 10^{-1}$	2.79	1.54
1620	9.5	938	73.6	$4.1 \cdot 10^{-3}$	$9.7 \cdot 10^{-1}$	2.79	1.53
3710	9.7	695	74.3	$7.5 \cdot 10^{-8}$	1.0	2.79	1.53
10300	9.7	480	74.4	$2.2 \cdot 10^{-16}$	1.0	2.78	1.53
31200	9.8	322	74.4	$\ll 1$	1.0	2.78	1.53
97400	9.8	213	74.4	$\ll 1$	1.0	2.77	1.53
307000	9.8	141	74.4	$\ll 1$	1.0	2.78	1.53
968000	9.8	93	74.4	$\ll 1$	1.0	2.78	1.53

ions. At sufficiently far distances, the sputtering effect balances this growth effect and results in the relaxation of the dust grain size.

The resulting ratio of the number of solid carbon to that of gaseous carbon is in the range 0.01–5%.

The characteristic final radius of the dust grains moving away into the interstellar medium is less than 0.01 μm.

The accuracy of the fits (3–7%) is quite satisfactory.

A more refined model of the dust shell is required in order to reduce the fitting error. Such a model should incorporate the details of the nucleation layer structure. The calculated values of $J_0 \, \Delta R_0$ can be used to search for the effective nucleation mechanism.

6. CONCLUSIONS

We propose a simple quasi-steady theory of the microstructure of a WR star dust shell. This theory allows to calculate the dust shell luminosity which can be compared with the observational data. For the special case of geometrically thin nucleation layer (which seems to be quite realistic) we have carried out a fitting procedure for the spectra of some late WC stars. We obtain the best-fit models and the main parameters of the dust shells including the nucleation rates. It turns out that the grains consist of graphite and have excessively small final sizes of 0.002–0.01 μm. The nucleation problem remains to be open. New observations of WR stars ranging from ultraviolet to infrared region are required to clarify the situation.

References

Allen, D. A., Swings, J. P. and Harvey, P. M. (1972). Infrared photometry of northern Wolf-Rayet stars. *Astr. Astrophys.* **20,** 333–336.

Cohen, J., Barlow, J. M. and Kuhi, L. V. (1975). Wolf-Rayet stars. VI. The nature of the optical and infrared continua. *Astr. Astrophys.* **40,** 291–302.

Danks, A. C., Dennefeld, M., Wamstecker, W. and Shaver, P. A. (1983). Near infrared spectroscopy and infrared photometry on a new WC9 star. *Astr. Astrophys.* **118,** 301–305.

Draine, B. T. and Lee, H. M. (1984). Optical properties of interstellar graphite and silicate grains. *Astrophys. J.* **285,** 89–108.

Gail, H.-P. and Sedlmayr, E. (1984). Formation of crystalline and amorphous carbon grains. *Astr. Astrophys.* **132,** 163–167.

Gehrz, R. D. and Hackwell, J. A. (1974). Circumstellar dust emission from WC9 stars. *Astrophys. J.* **194,** 619–622.

Hackwell, J. A., Gehrz, R. D. and Grasdalen, G. L. (1979) Dust formation around HD 193793. *Astrophys. J.* **234,** 133–139.

Kikoin, I. K. (1976) *The tables of the physical quantities,* Atomizdat, Moscow, 1008 p.

Nugis, T. (1977). The study of the Wolf-Rayet star HD 192163. *Publ. Tartu Astrofiz. Obs.* **45,** 70–112.

Nugis, T. (1991). Chemical composition in the envelopes of different WR subtypes. In *Wolf-Rayet Stars and Interrelations with Other Massive Stars in Galaxies,* K. A. van der Hucht and B. Hidayat eds, Reidel, Dordrecht, pp. 75–80.

Pitault, A., Epchtein, N., Gomez, A. E. and Lortet, M. C. (1983). Infrared photometry of southern Wolf–Rayet stars. *Astr. Astrophys.* **120,** 53–57.

Van der Hucht, K. A., Conti, P. S., Lundstrom, M. I. and Stenholm, B. (1981). The sixth Catalogue of galactic Wolf–Rayet stars, their past and present. *Space Sci. Revs.* **28,** 227–306.

Williams, P. M., Beattie, D. H., Lee, T. J., Stewart, J. M. and Antonopoulou, E. (1978) Condensation of a shell around HD 193793. *Mon. Not. R. astr. Soc.* **185,** 467–472.

Williams, P. M., Longmore, J., van der Hucht, K. A., Talavera, A., Wamsteker, W. M., Abbott, D. C. and Telesco, C. M. (1985) Condensation of dust around the WC7 star HD 192641 (WR137). *Mon. Not. R. astr. Soc.* **215,** 23P–29P.

Williams, P. M., van der Hucht, K. A. and The, P. S. (1987). Infrared photometry of late-type Wolf–Rayet stars. *Astr. Astrophys.* **182,** 91–106.

Williams, P. M., van der Hucht, K. A., Pollock, A. M. T., Florkowski, D. R., van der Woerd, H. and Wamsteker, W. M. (1990) Multi-frequency variations of the Wolf–Rayet system HD 193793. I. Infrared, X-ray and radio observations. *Mon. Not. R. Astr. Soc.* **243,** 662–684.

Zubko, V. G., Marchenko, S. V. and Nugis, T. (1992). Dust in the expanding Wolf–Rayet star atmospheres. I. An analysis of infrared observations and possible dynamical mechanism of dust grain growth. *Astron. Astrophys. Transac.*